

# Recognition of Blister Blight Disease in Tea Leaf Using Fully Convolutional Neural Networks

L.Leema priyadarsini, D.Femi

**Abstract:** Tea plantation contributes significantly to the agricultural economy of India. Automatic tea leaf disease detection is beneficial when compared to manual detection which is not only a tedious grueling task but also less accurate and time consuming. This paper presents an alternative image segmentation technique that can be used for automatic detection and classification of blister blight diseased tea leaf using a fully convolutional neural network (CNN) based method to segment blisters in a tea leaf image. The suggested technique proves to be beneficial in monitoring large fields of tea crops.

**Index Terms:** Segmentation technique, blister blight, convolutional neural network.

## I. INTRODUCTION

Deep learning is inevitably the leading machine learning tool in the general imaging and computer vision domains. In particular, convolutional neural networks (CNNs) have ended up being useful assets for a wide scope of computer vision tasks. Deep CNNs consequently learn mid-level and abnormal state reflections obtained from crude information (e.g., pictures). Recent results indicate that the nonexclusive descriptors extracted from CNNs are extremely effective in object recognition and localization in natural images. The primary advantage of neural networks over traditional machine learning algorithms is that CNNs do not need hand-crafted features, making it applicable to a diverse set of problems when it is not obvious what features are optimal.

Segmentation in jpeg images is an exigent task for various reasons: (1) blister boundaries are often not well defined, particularly on JPEG images, and (2) clinical quality of JPEG images may possess low resolution and often have imaging artifacts. Therefore there is an inherent reliability challenge associated with blister segmentation.

## II. METHODOLOGY

### A. Image Acquisition

Image acquisition is the foremost step that demands capturing jpeg images of diseased leaves. Since the blisters in tea leaves are highly variable in terms of size (pinhole-size spots on young leaves) and location (underside of leaves), it is practically very difficult to capture them through manual

inspection. So the use of digital camera placed at regular spacing in the tea plantation area will acquire good quality jpeg images to be given to the image segmentation system.

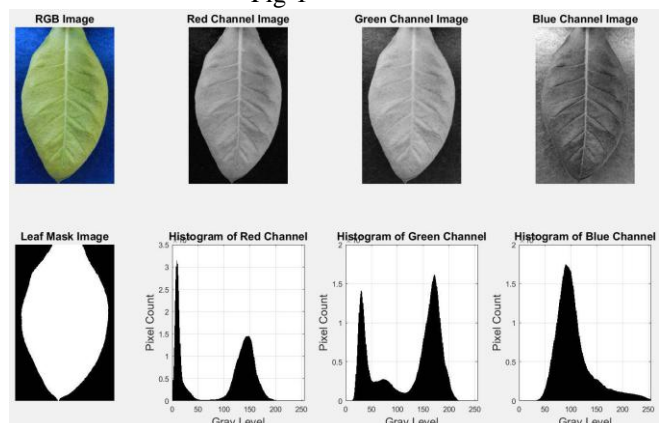
### B. Image Segmentation

Next preprocessing of input image is done so as to improve the quality of image and to expel the undesired distortion. They are then corrected for any intensity in homogeneity. Clipping of the leaf image is performed to get the interested image region and then by utilizing the smoothing filter, image smoothing is performed. To improve the contrast image enhancement can also be done. Masking is performed on the pixels based on the pre-computed threshold value to isolate the area of interest from the entire image. Thresholding is the simplest method of segmentation. From a grayscale image, thresholding can be used to create binary images. In this step, mostly the green hue pixels are masked. In this, we computed a threshold value that is used for these pixels. Then in the following way mostly green pixels are masked: if pixel intensity of the green component is less than the pre-computed threshold value, then zero value is assigned to the red, green and blue components of this pixel. Image segmentation includes feature extraction.

### C. Feature Extraction

Over the traditional gray-scale representation, in the visible light range, the use of color image features paves way to an additional feature for image characteristic. There are three vital mathematical processes in the color co-occurrence distribution method. The first of which is the conversion of the RGB images of leaves into HSI (Hue Saturation Intensity) color space representation.

Fig-1



In the HSI representation, hue component represents color determined by angles ranging from 0 to 360 degrees. The saturation component, reflects the

Revised Manuscript Received on July 05, 2019

L.Leema priyadarsini, Department of Computer Science and Engineering, Veltech Rangarajan Dr.Sakunthala R & D Institute of Science and Technology, Chennai,India.

D.Femi, Department of Computer Science and Engineering, Veltech Rangarajan Dr.Sakunthala R & D Institute of Science and Technology, Chennai,India.



# Recognition of Blister Blight Disease in Tea Leaf Using Fully Convolutional Neural Networks

amount of purity (distance from vertical axis) ranging from 0 to 1 where closer the distance, paler will be the color. Also the intensity component represents brightness (distance from bottom) ranging from 0 to 1. The histogram of the resulting RGB channels are evident from Fig 1. After completion of this procedure, in order to generate a color co-occurrence distribution or matrix, each pixel map is used, which results into three color co-occurrence distributions, one for each of H, S, I. The obtained co-occurrence distribution gives the distribution of co-occurring pixel values or colors at a given offset( $\delta a, \delta b$ ) which can be applied to any pixel in the image (ignoring edge effects). Hence an image with  $p$  different pixel values will produce  $p \times p$  co-occurrence distribution for the given offset. So  $D(i, j)^{\text{th}}$  value of the co-occurrence distribution indicates the number of times in the image, the  $i^{\text{th}}$  and  $j^{\text{th}}$  pixel values occur in the relation given by the offset( $\delta a, \delta b$ ) shown in the below equations (1) and (2)

$$(\partial a, \partial b) = i \quad (1)$$

$$I(a + \partial a, b + \partial b) = j \text{ otherwise} \quad (2)$$

Subsequently, to quantify the perceived texture (information about the spatial arrangement of color or intensities in selected region of image) some of the features called as texture features, which include local homogeneity, contrast, cluster shade, energy, and cluster prominence are computed for the input image as shown in the equations (3),(4) and (5).

$$LH = \sum_{i,j=0}^{N-1} D(i, j) / (1 + (i - j)^2) \quad (3)$$

$$Contrast = \sum_{i,j=0}^{N-1} (i, j)^2 D(i, j) \quad (4)$$

$$Energy = \sum_{i,j=0}^{N-1} D(i, j)^2 \quad (5)$$

The feature values for the tea leaves thus obtained from the co-occurrence distribution are compared with the corresponding feature values stored in the feature dataset. Further convolutional neural network is used for classification supported by parameter optimization.

## III. IMPLEMENTATION

### A. Implementation Details

As the typical convolutional neural network architecture for image processing consists of a series of layers of convolution filters, interspersed with a series of data reduction or pooling layers, the convolution filters are applied to small patches of the input image. The convolution layer is the foremost layer that takes the input image (matrix with pixel values) and selects a smaller matrix from it called as a filter or kernel. Multi-channel patches are first independently passed through convolutional filter banks, then a fully connected (FC) layer is applied to predict the voxel-wise membership at the center of the patches from the concatenated outputs of the filters. In the proposed architecture, multi-channel 2D patches are convolved with multiple filter banks of various sizes and the outputs of the convolutional pathways are concatenated.

Table I

Filter Bank	Type	No. of Filter s	Filter size	Parameters	No. of paramet ers
1	Convolution	128	$3^2$	$3 \times 3 \times 128$	1152
2	Convolution	64	$5^2$	$5 \times 5 \times 128 \times 64$	204800
3	Convolution	32	$3^2$	$3 \times 3 \times 64 \times 3$ 2	18432

After concatenation, instead of an FC layer to predict the membership or probability of the center voxel of the  $p1 \times p2$  patch, we add another convolutional pathway that predicts a membership value of the whole  $p1 \times p2$  patch. Note that with variable pad sizes (refer Table 1), the sizes of the input and outputs of the filters are kept identical to the original jpeg image patch size. The training memberships are generated by simply convolving the manual hard segmentations with a  $3 \times 3$  (denoted 32) Gaussian kernel. It has been observed that larger patches produce more accurate segmentations compared to smaller patches, and determined that a  $35 \times 35$  patch produced the best results based on the dataset.

Improved segmentation results were achieved using a set of 5 convolutional filter banks with decreasing numbers of filters in one convolutional pathway, as shown in the Table I. The optimal number of filter banks in a pathway were also estimated from a validation strategy discussed earlier. Each convolution is followed by a rectified linear unit. Our experiments showed that smaller filter sizes such as 32 and 52 generally produce better segmentation than bigger filters such as 72 and 92. We hypothesize that since blisters boundaries are often not well defined, small filters tend to capture the boundaries better. Also the number of free parameters (9 for 32) increases for larger filters (49 for 72), which in turn can either decrease the stability of the result or incur overfitting. However, smaller filters may perform worse for larger blisters. Therefore we empirically used a combination of 32 and 52 filters based on our validation set. It is evident that, a major difference in the network architecture proposed here in contrast to other popular convolutional neural network based segmentation method is the use of a convolutional layer to predict membership functions.

### B. Metrics

The metrics used are: Dice coefficient, blister false positive rate (BFPR), and positive predictive value (PPV) to compare segmentations. The manual and an automated binary segmentation are denoted by M and A respectively. Dice is a voxel-wise overlap measure. Since the blisters are often small and their total volumes are typically very small compared to the whole leaf volume, Dice can be affected by the low volume of the segmentations. Therefore Blister false positive rate is defined based on distinct blister counts. A distinct blister is defined as an 10-connected object, although such a description of blister may or may not be biologically accurate. Blister false positive rate is the number of blisters in the automated segmentation that do not overlap with any blister in the manual segmentation, divided by the



total number of blisters present in the automated segmentation. Any two blisters are considered overlapped when they share at least one voxel. Positive predictive value is defined as the ratio of true positive voxels to the total number of positive voxels.

### C. Parameter Optimization

The three vital user selectable parameters of the proposed network are: (1) patch size, (2) number of filter banks in a convolutional pathway, and (3) the final threshold to create hard segmentations from memberships. The validation strategy to optimize the membership threshold, the convolutional neural network is trained with  $35 \times 35$  patches and the generated memberships were segmented with thresholds from 0.05 to 0.85 with an increment of 0.05. Next we varied the depth of a convolutional pathway from 2 to 6 filter banks while keeping the number of filters as a multiple of 2, with the last filter bank having 8 filters. Patch size is another important parameter of the network. In computer vision applications such as object detection, usually a whole 2D image is used as a feature. As the patch sizes increases, the false positives that are mostly observed in the cortex tend to decrease. Although training was performed with different patch sizes, the memberships were generated slice by slice, as the trained model consisted only of convolutions and did not need any information about patch sizes.

## IV. RESULTS AND DISCUSSION

### A. Results

The proposed methodology is a simple end-to-end fully convolutional neural network based technique to segment blisters from multi-contrast jpeg images. Even though the network does not have any fully connected layers, after training it takes only a couple of seconds to segment blisters on a new image. We used large 2D patches for our experiment in comparison to isotropic. The rationale behind using large anisotropic patches is twofold. First, experiments with full 3D isotropic 93 or 113 patches showed little or no improvement in Dice and led to increased false positives, with memberships similar to the one with  $13 \times 13$  patches. Larger isotropic patches, e.g. 193 or 253, showed inferior segmentation, and in some cases, optimization did not converge. The reason is that the jpeg images in the test datasets had inherently low resolution in the inferior-superior direction, 2:2 mm and 4:4 mm compared to in-plane resolution of  $0.82 \times 0.82$  mm.

Therefore 2D axial patches capture the high resolution in-plane information that represents the original thick axial slices. Also, the blisters are usually focal and small in size, unlike other leaf regions. Therefore a very large isotropic patch around a small blister can include superfluous information about the blister, which can increase the amount of false positives. However this method requires a large number of training patches. To further improvise the metrics such patch rotation can be done on the training patches.

### B. Discussions

Patch rotation being a standard data augmentation technique, rotates the training patches by  $45^\circ$ ,  $90^\circ$ ,  $135^\circ$  and  $180^\circ$  in the axial plane and appends it to the training patch set in addition to the non-rotated patches. This showed only 1 to

2% increase in average Dice coefficients with rotated patches at the cost of significantly more memory and training time, indicating that the network is already sufficiently generalizable with the original training data. Therefore we did not use rotated patches in the final segmentation. It is however essential to understand the full scope of performance improvement with respect to the available training data and other augmentation techniques, such as patch cropping or adding visually imperceptible jitters to images.

## REFERENCES

1. Snehasis Roy, John A. Butmana,b, Daniel S. Reichb,c,d , Peter A. Calabresid, Dzung L. Phama "Multiple Sclerosis Lesion Segmentation from Brain MRI via Fully Convolutional Neural Networks" Elsevier, March 2018.
2. Vijai Singh, A.K. Misra, "Detection of plant leaf diseases using image segmentation and soft computing techniques" Information Processing in Agriculture, Elsevier 2017.
3. S. B. Ullagaddi, Dr. S.Vishwanadha Raju, "A review of techniques for Automatic detection and diagnose of mango pathologies" International Journal of Engineering and Computer Science ISSN: 2319-7242 Volume 5 Issue 5 May 2016
4. Kamlesh Golhani , Siva K. Balasundram,, Ganesan Vadamalai , Biswajeet Pradhan, "A review of neural networks in plant disease detection using hyperspectral data" Information Processing in Agriculture ,Elsevier 2018.
5. Asaram Pandurang Janwale, "Plant leaves image segmentation techniques: A Review", International Journal of Computer Science and Engineering, June 2017.
6. L.Leema priyadarsini, D.Femi , S.Thylashri , K.Prema, "Recognition Of Image Verification Using Lossless Predictive Coding", International Journal of Engineering & Technology, Vol .7, Issue 2.19, pp. 84-86, 2018.
7. K.Prema, L.Leema priyadarsini, C.Shyamala Kumari, S.Florence, "Human Intention detection with facial expression using video analytics", International Journal of Engineering and Technology, Vol .7, Issue 2.4, pp. 14-16, 2018
8. C.Shyamala Kumari, S.Florence, L.Leema priyadarsini., "LIFI- the future of wireless Technology", International Journal of Engineering and Technology, Vol .7, Issue 2.4, pp. 17-19, 2018.
9. S.Florence, C.Shyamala Kumari, L.Leema priyadarsini, "Smart health monitoring system based on internet of things with big data analytics and wireless networks", International Journal of Engineering and Technology, Vol .7, Issue 1.7, pp. 107-111, 2018
10. K.Prema, L.Leema priyadarsini, C.Shyamala Kumari, S.Florence, "Survey in detecting human beings behavior under video surveillances and its applications", Journal of Computational and Theoretical Nanoscience, Vol 15, pp.1-3,2018

## AUTHORS PROFILES



**L. Leema Priyadarsini** M.E, Software Engineering, Assistant professor, VelTech Rangarajan Dr.Sagunthala R&D Institute of Science and Technology, Avadi, Chennai, Tamilnadu, India. Published Papers in Scopus Indexed Journals on topics "Recognition of Image Verification using Lossless Predictive Coding", International Journal of Engineering and Technology, Vol .7, Issue 2.4, pp. 17-19, 2018. "Predicting implicit search behaviors using log analysis", International Journal of

Engineering and Technology, Vol .7, Issue 1.7, pp. 91-95, 2018. "Human Intention detection with facial expression using video analytics", International Journal of



## Recognition of Blister Blight Disease in Tea Leaf Using Fully Convolutional Neural Networks

Engineering and Technology, Vol .7, Issue 2.4, pp. 14-16, 2018, "LIFI- the future of wireless Technology", International Journal of Engineering and Technology, Vol .7, Issue 2.4, pp. 17-19, 2018. "Smart health monitoring system based on internet of things with big data analytics and wireless networks", International Journal of Engineering and Technology, Vol .7, Issue 1.7, pp. 107-111, 2018. Membership in "Institute of Electrical and Electronics Engineers."



D FEMI received her BE degree in Computer Science and Engineering from Anna University, Chennai in 2014. She has completed his Masters degree in CSE from Anna University, Chennai in 2016. Now she is currently working as Assistant Professor in the Department of Computer Science and Engineering at Vel Tech Rangarajan Dr.Sagunthala R&D Institute of Science and Technology, Chennai, India. Her

area of interest is image processing, wireless sensor networks, and Data Mining.



Published By:  
Blue Eyes Intelligence Engineering  
& Sciences Publication